Patterning of Human Dental Arch Wire Blanks Using a Vector Quantization Algorithm

Kyoko Fujita, DDS[a]; Kenji Takada, DDS, PhD[b]; Gu QianRong[c]; Tadashi Shibata, PhD[d]

Abstract: We objectively and automatically classified arch wire blank forms represented by a series of facial surface points on tooth crowns in human adults with normal occlusions using a vector quantization algorithm on the basis of the generalized Lloyd algorithm. We investigated also the descriptive dental arch form parameters that were most effective in distinguishing the classified groups of dental arch wire blanks and examined if they were associated with specific anatomical traits. Dental casts, taken from 79 adults with complete dentitions, were laser scanned with a computer-assisted stereotaxic device. Coordinates of the tooth crown points (FA points) were measured for each dental arch expressed as a vector having positional elements in a series of 14 FA points and categorized into several codes (ie, patterns) according to the similarity of the quantized vector patterns. We found that classifying the dental arches into four patterns maximized the difference between arch wire blank patterns. The classified patterns were differentiated by a gradual broadening of the interarch widths posterior to the lateral incisor. The code with the narrowest arch had the longest coronal arch, whereas the code with the widest arch had the shortest coronal arch ($P < .01$). The interpremolar and intermolar basal arch widths determined for the code showing the widest arch were significantly greater than those for the code with the narrowest width ($P < .01$). (*Angle Orthod* 2002;72:285–294.)

Key Words: Arch wire; Dental arch; Generalized Lloyd algorithm; Occlusion; Vector quantization

INTRODUCTION

To date, orthodontic treatments of most patients with permanent dentitions use a straight edgewise appliance, with an arch wire as one of the most essential elements. The form of the arch wire blank is designed to move teeth into an optimal arch form. Afterwards, the arch wire blank is engaged into channels of the orthodontic attachments located on the crown points (FA points) to move the teeth. The assumption supporting this paradigm is that the form of the arch wire blank represents an optimal dental arch form. There is, however, no consensus on the optimal dental

arch form to be achieved as the result of treatment. In orthodontic practice, therefore, a fundamental question is how practitioners make the correct design for the arch or how they select the appropriate form from arch wire blanks.

Though we must admit that each patient should be given individualized normal dental arch forms at the end of treatment, it would be reasonable to stereotype arch wire blanks constructed from individuals with normal dental arch forms into a few sets of patterns according to their geometric similarities. There is no objective chairside rationale that explains why an arch wire with a specific arch form is chosen. Previous studies, using conventional anatomic points on the incisal edges and molar cusp tips, classified dental arch forms from individuals with various types of occlusions into various mathematical forms such as paraboloid,[2,3] catenary curves,[4] elliptic curves,[3] conic sections,[5,6] spline curves,[7] and the beta function,[8] all of which give us an idea of how the dental arch form might be shaped. Despite their biological significance, however, they do not provide us with clinical evidence of appropriate forms of arch wire blanks. Teeth's FA points give direct representations of arch wire blank forms.

Uzuka and his associates[9] applied a polynomial curve fitting to a series of FA points on laser-scanned three-dimensional dental casts[10,11] to determine optimal approximates of dental arch forms. They found that 50% of the

[a] Clinician, Department of Orthodontics, Osaka University Dental Hospital, Osaka, Japan.

[b] Professor and Chair, Department of Orthodontics and Dentofacial Orthopedics, Graduate School of Dentistry, Osaka University, Osaka, Japan.

[c] Department of Frontier Informatics, Graduate School of Frontier Science, The University of Tokyo, Tokyo, Japan.

[d] Professor, Department of Frontier Informatics, Graduate School of Frontier Science, The University of Tokyo, Tokyo, Japan.

Corresponding author: Kenji Takada, DDS, PhD, Department of Orthodontics and Dentofacial Orthopedics, Graduate School of Dentistry, Osaka University, 1-8 Yamadaoka, Suita, Osaka, Japan 565-0871

(e-mail: ktakada@dent.osaka-u.ac.jp).

dental arch forms in subjects having normal occlusion were best expressed by the fourth-order polynomial curves, 15% by the second-order polynomials, and 13% by the sixth-order polynomials. Their findings suggest that the form of the arch wire blank representing the normal dental arch form is not a single entity.

What we should recognize in the mathematical modeling of dental arch forms is that dental arches that are identified to have the same type of mathematical form of function do not necessarily share the same pattern. Similarly, polynomials with the same order do not always show the same geometric patterns. They may differ depending on the coefficients of each term in the function. Also, the differences in orders between polynomial functions do not give us a concrete image of how arch wire blank forms are designated mathematically. Classification by the type of function does not classify the dental arch wire blank forms according to similarity of the patterns.

It is important to investigate whether the arch wire blank forms constructed from normal dental arch forms are classified into subtypes according to similar geometric patterns if we are to predict at the outset the dental arch form that should be achieved at the end of orthodontic treatment. Furthermore, it is important to determine factors that distinguish subtypes and to examine whether there is any association between arch blank forms and the morphology of the surrounding structures and teeth.

The purposes of this study are (1) to classify objectively and automatically dental arch wire blank forms represented by the FA points in humans with normal occlusions using the vector quantization algorithm[12] based on the generalized Lloyd algorithm,[13] (2) to investigate the descriptive parameters of the dental arch wire blank form that are most effective in discriminating between groups of dental arches, and (3) to discuss whether the classified dental arch wire blank forms are associated with specific dentoskeletal morphological traits.

MATERIALS AND METHODS

Dental casts were made of 79 healthy Japanese adult volunteers (mean age, 22 years 6 months; range, 19 years 0 months–37 years 0 months) with complete dentitions; Class I molar, canine, and incisor relationships;[2,14] tight intercuspation of teeth; and no discernible crowding of the teeth. The patients were selected for the study by visual inspection.

Three-dimensional data acquisition

Dental casts were laser scanned with a personal computer-assisted stereotaxic device (Surflacer VMS150R-D, UNISN Inc, Osaka, Japan). Upper and lower anterior segments of the dentitions were scanned from three directions, whereas the posterior segments were recorded from five directions, with scanning pitches of 0.20 mm in the X-axis and 0.25 mm in the Y-axis. The X-axis was parallel to the

projected direction of the laser beam and the ground, whereas the Y-axis was perpendicular to the beam and parallel to the ground. Any arbitrary point on the dental cast from which the laser beam projection originated was defined as the origin. A line perpendicular to the X- and Y-axes was defined as the Z-axis. The digitized data were synthesized to reconstruct a three-dimensional surface model of the entire dentitions and their adjacent structures. A detailed description of the performance characteristics including measurement accuracy of the current data recording system has been reported elsewhere.[9] The measurement error was smaller than 0.05 mm. The recorded data were transferred to a workstation (Silicon Graphics O2, Silicon Graphics Inc, Mountain View, Calif. for subsequent computation and analysis with a software program (Surfacer, Version 9.0, Structural Dynamic Research Corp, Maryland Heights, Missouri).

Measurement of FA points

The FA point was defined as the midpoint on the facial axis of the clinical crown (FACC). It divides the most prominent point on the central lobe of the facial axis of all clinical crowns except for the molar teeth.[1] The FACC was determined on the mesiobuccal groove of the molar teeth and measured on the digitized image of the dental cast. The midpoint between the mesiodistal midpoints on the central incisor edges in each dental arch and the mesiopalatal cusp tips of the upper first molars bilaterally (distobuccal cusp tips of the lower first molars bilaterally in the lower arch) were employed as reference points to provide reference planes (the occlusal planes) in each dental arch. A new three-dimensional coordinate system was then created with the image data where the midpoint between the FA points of the right and left central incisors was defined as the origin in each dental arch. The three-dimensional coordinates of the FA points were measured against the coordinate system. The X-axis was defined as a line parallel to the first molar points through the origin in each dental arch. The Y-axis was defined as a line perpendicular to the X-axis through the origin and parallel to the reference plane, while the Z-axis was defined as a line perpendicular to the X-Y plane through the origin.

Patterning of dental arch wire blanks by vector quantization

In the present study, we attempted to classify a set of dental arches into several patterns by vector quantization based on the generalized Lloyd algorithm.[13] A detailed description of the vector quantization is provided in the Appendix of this article.

Each dental arch form projected onto the occlusal plane was mathematically expressed as a 28-dimensional vector (or a vector having 28 elements) that was composed of X and Y coordinates of the 14 FA points.
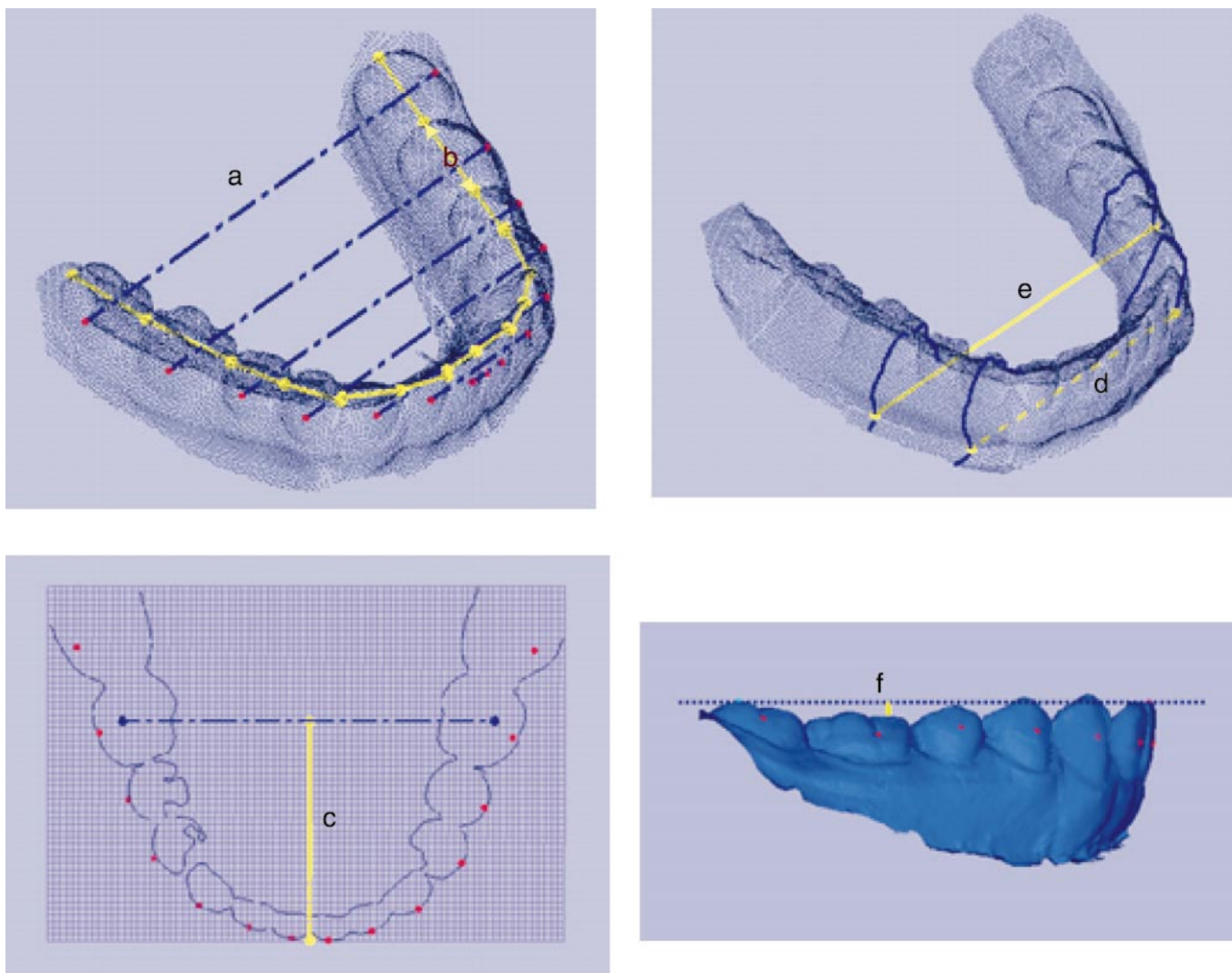
FIGURE 1. Dental cast measures employed in the present study. For simplicity, only the lower dental arch is exemplified. (a) Top left, yellow chain lines: coronal arch widths, the distance between the FA points of the same kind of teeth. (b) Top left, green lines: mesiodistal crown widths of each individual tooth. (c) Top right, green line: coronal arch length. (d, e) Bottom left, green lines: interpremolar basal arch width and intermolar basal arch width. Coronal sections of teeth and their adjacent apical base contours are shown by blue lines. (f) Bottom right: the deepest point on the curving lines of dental arch connecting the incisor edges and cusp tips of the canine, premolar, and molar teeth projected onto the midsagittal plane. For the upper molars, the palatal cusps were employed, and for the lower molars, the buccal cusps were chosen.

Calculations were made to classify each set of the upper and lower dentitions into two, three, four, five, and six subcategories or code sets, ie, two to six code vectors, with a weighting coefficient of 1.0 assigned to each element of the vector. The number of code sets was selected arbitrarily. Each trial classified the set of dental arch forms into code sets two, three, four, five, or six. Subsequently, we calculated the average deviations, which decreased with the increase in the number of codes. The rates of decrease gradually reduced as the code number increased. Accordingly, the optimal number of code sets was represented by the dental arch patterns with the greatest reduction in average deviations.

For the code set with the optimal number, we assigned heuristically the weighting coefficients of 0.5, 1.0, 1.5, and 2.0 to each vector element and teeth of the same kind weighted equally, thus providing 4^{14} combinations of code vectors. All weighting combinations were applied to each of the 79 dental arch forms to perform the vector quantization. In addition, a polynomial curve fitting was made for each coded dental arch to provide R^2 values and probabilities of significance for coefficients for each term. Also, we determined the frequency of paired upper and lower codes and proportions of each code with respect to the total sample size for the upper and lower dental arches. Finally, we measured the mean distances (and their standard deviations) in the lateral direction between the FA points of the paired upper and lower codes at the canine and the first molar teeth.

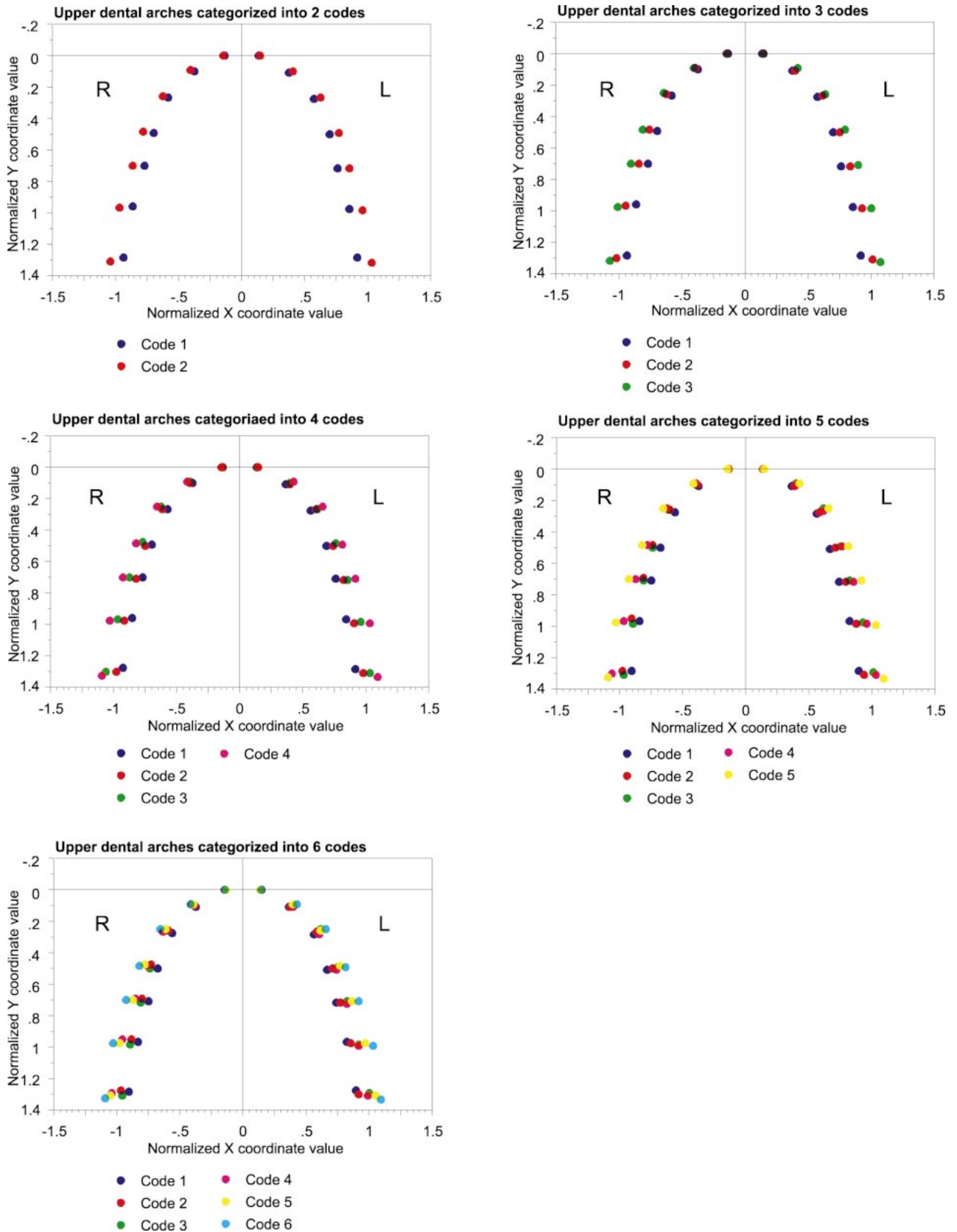To investigate how the dentoskeletal characteristics of the

FIGURE 2. Computer plots of dental arch forms expressed by a series of FA points. (a) Upper dental arch, (b) lower dental arch. Plots were made for each of the codes of dental arch form patterns that were computed by assuming a number of codes (arch form patterns) ranging between two and six.
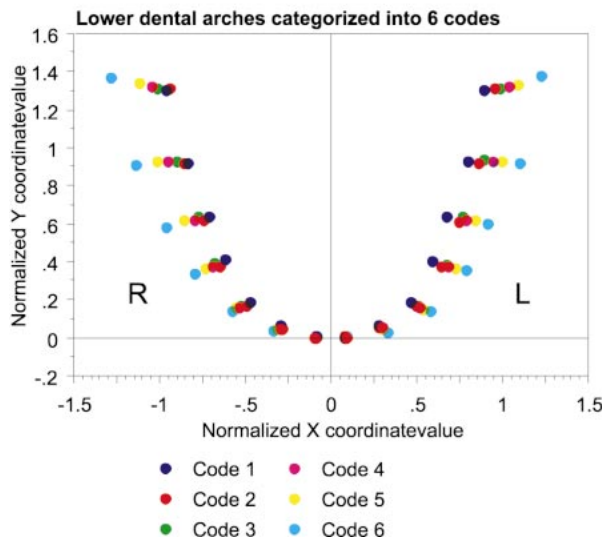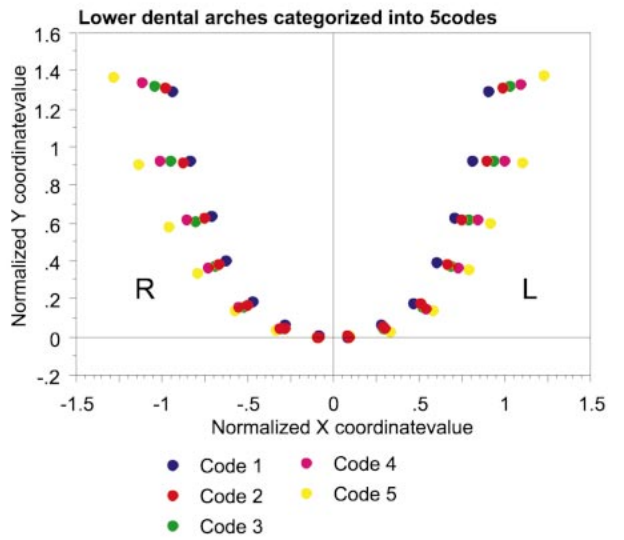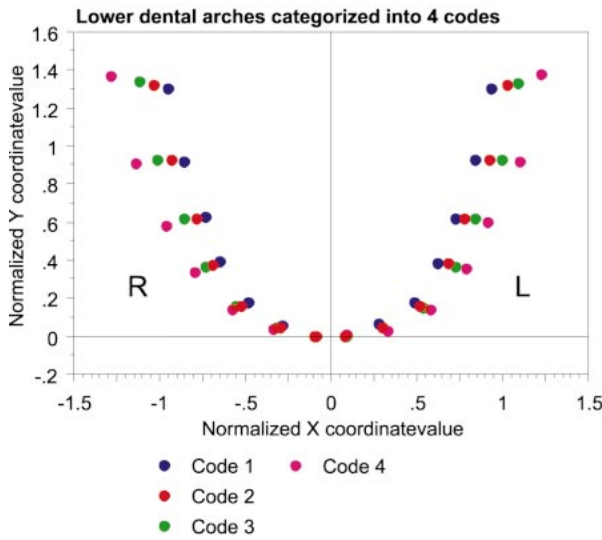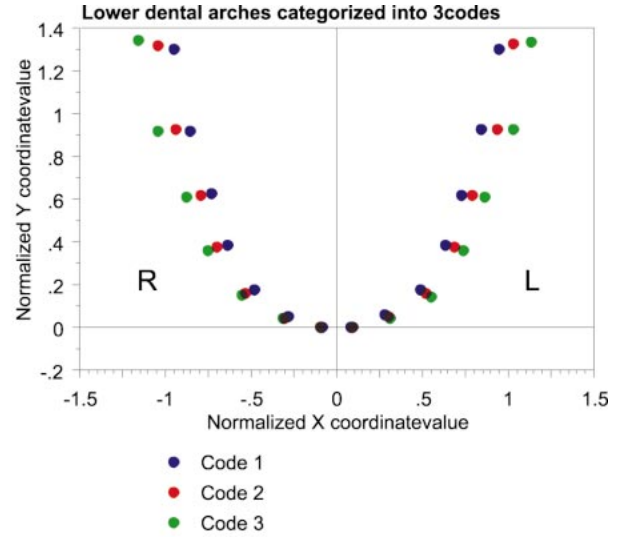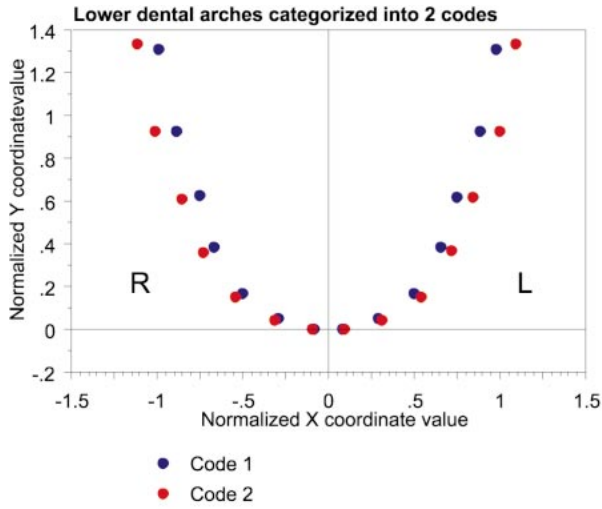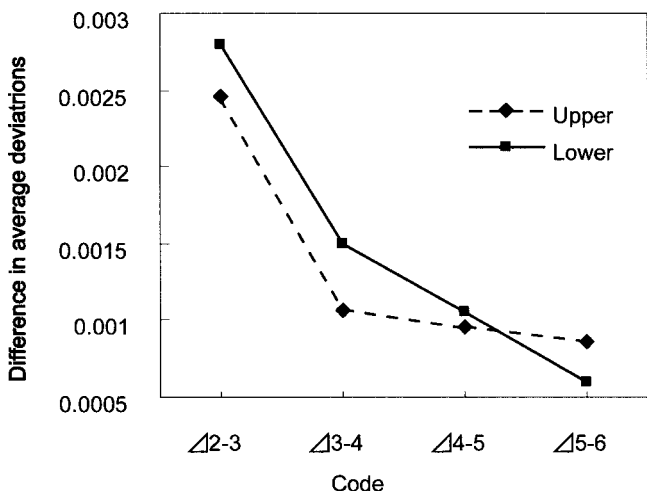
FIGURE 2. Continued.

FIGURE 3. Amount of decrement in average deviation between a designated number of codes and its preceding number of codes. δ3-2, differences in average deviation between the pattern categorizations into three and two codes. The remaining differences follow an identical rule. Solid line, upper dental arch; dotted line, lower dental arch.

coded dental arch form patterns are distinguished, we measured the coronal arch widths, the basal (skeletal) arch widths, the depths of the curve of Spee in the lower dental arch along with the accentuated curve of Spee in the upper dental arch, the mesiodistal crown widths of each individual tooth, and the coronal arch length. Then we compared the clustered codes using a Mann-Whitney's *U*-test. For a test of significance, *Z*-values were adopted for each mesiodistal crown width and depths of the dental arches, whereas *U*-values were employed for the remaining variables. The coronal arch widths indicate the distances between the right- and left-side FA points on the same kind of teeth. The coronal arch length was defined as a distance from the center of the midpoints on the central incisor edges to the mesiopalatal cusp tips of the bilateral upper first molars and distobuccal cusp tips of the bilateral lower first molars projected onto the aforementioned reference plane in each dental arch. The basal arch widths were defined as the distances between the innermost points at the buccal folds on a plane including the buccal cusp tips of the first premolar teeth (or the mesiobuccal cusp tips of the first molar teeth) and perpendicular to the reference plane (Figure 1).

RESULTS

There was a trait common to all outputs of sets of dental arch forms that corresponded to the designated number of codes. For any designated code number, the dental arch forms were differentiated by a gradual broadening of the interarch widths posterior to the lateral incisor teeth (Figure 2).

Remarkably, the amount of decrement for the average deviations showed the most change when classifying dental arch form patterns into four codes (Figure 3). Accordingly,

TABLE 1. Frequencies of Paired Upper and Lower Codes and Proportions of Each Code (% in Parentheses) With Respect to the Total Sample Size for the Upper and Lower Dental Arches Determined for the Four-Code Set[a]

	Upper					
	Code 1	Code 2	Code 3	Code 4	Total	(%)
Lower						
Code 1	19	5			24	(30.4)
Code 2	4	17	10	2	33	(41.8)
Code 3		1	13	5	19	(24.0)
Code 4				3	3	(3.8)
Total	23	23	23	10	79	(100)
(%)	(29.1)	(29.1)	(29.1)	(12.7)	(100)	

[a] Note that the code numbers in the upper arch do not necessarily correspond to the code having the same number in the lower arch because coding was made independently for each dental arch.

the optimal difference in the coded patterns was obtained by classifying the arches into four codes.

There were several combinations of weighting coefficients that showed the minimal average deviation values. In other words, there was no sole combination of weighting coefficients that served to maximize the difference between coded arch forms. Differences between the minima and the maxima of the average deviation were <0.01 mm for both of the upper and lower dental arches, and equal weighting of 1.0 on all teeth was employed. The fourth-order polynomials provided the best fittings for both the upper and lower arches.

Proportions of upper and lower dental arches given to each code compared with those given to the total sample size and frequencies of paired upper and lower codes are given in Table 1. In the upper dental arch, codes 1, 2, and 3 showed almost equal proportions of 29%, whereas code 4 exhibited the lowest proportion (13%). In the lower dental arch, the code 2 showed the highest proportion (42%), which was followed by code 1 (30%), code 3 (24%), and code 4 (4%). The majority of the lower code 1 occluded with the upper code 1 in 19 cases out of 24. Similarly, the remaining lower code vectors most frequently corresponded with the upper codes of the same numbers. The remaining paired dental arches showed combinations with neighboring codes.

Mean distances in the lateral direction (and their standard deviations) between the FA points of the paired upper and lower codes at the canine and the first molar teeth are given in Table 2.

The FA points on the upper and lower canine teeth ranged between 3.6 mm (the combination of the upper code 2 and the lower code 3, one case) and 5.0 mm (upper code 2 and lower code 1, five cases) apart laterally. Upper and lower canines were located 4.4 mm (code 1, 19 cases), 4.4 mm (code 2, 17 cases), 4.1 mm (code 3, 13 cases), and 4.2 mm (code 4, three cases) apart for the upper and lower arch pairs, which showed the highest frequencies. FA points on

TABLE 2. Mean Distances in the Lateral Direction (and Their Standard Deviations) Between the FA Points of the Paired Upper and Lower Codes at the Canine and the First Molar Teeth

	Upper							
	Code 1		Code 2		Code 3		Code 4	
	Mean (mm)	SD	Mean (mm)	SD	Mean (mm)	SD	Mean (mm)	SD
Lower								
Canines								
Code 1	4.4	0.9	5.0	0.8				
Code 2	3.8	0.7	4.4	0.9	4.6	0.5	4.5	0.5
Code 3			3.6	0.1	4.1	0.7	4.5	0.9
Code 4							4.2	0.9
First molars								
Code 1	2.7	1.1	2.8	0.8				
Code 2	2.4	1.6	2.3	1.0	2.9	0.9	2.9	0.8
Code 3			0.9	0.2	2.5	1.1	2.7	0.6
Code 4							3.0	0.8

the molar teeth ranged between 0.9 mm (the combination of the upper code 2 and the lower code 3, one case) and 3.0 mm (upper code 4 and lower code 4, three cases) apart. Furthermore, the upper and lower molars were located laterally 2.7 mm (code 1, 19 cases), 2.3 mm (code 2, 17 cases), 2.5 mm (code 3, 13 cases), and 3.0 mm (code 4, three cases) apart in the upper and lower arch pairs with the highest frequencies.

The code 1 subgroup exhibited the longest actual mean coronal arch length (upper 32.8 mm, lower 29.8 mm) of the four coded subgroups, which was significantly longer ($P < .01$) than that of the code 4 subset with the shortest coronal arch length (upper 29.7 mm, lower 25.9 mm). Significant differences were not found for the mesiodistal crown width variables between the code 1 and code 4 in either dental arch. The sums of the tooth crown diameters from the second molar tooth on one side to that on the other side did not differ significantly between the code 1 and code 4. Comparisons of the interarch widths and of the depths of the arches between code 1 (narrowest dental arch form) and the code 4 (widest dental arch form) subsets are presented in Table 3. Significant ($P < .01$) differences were determined between the two codes for the coronal arch widths posterior to the lateral incisors for each of the upper and lower arches. The interpremolar and intermolar basal (ie, skeletal) arch widths in the upper and lower arches of code 4 subset were significantly ($P < .01$) greater than those of the code 1 subset. Finally, neither of the depth of curved occlusal planes in the maxilla and the mandible differed between code 1 and code 4.

DISCUSSION

Previous studies formulated human dental arch forms in individuals with good occlusions into mathematical forms.[2–7,9] Efforts were made to fit each individual form with a specific

TABLE 3. Means and Standard Deviations for Coronal Arch Widths, Basal Arch Widths, and Depths of Dental Arches and Significances of Mean Differences Between the Code 1 Sample (n = 23 for the Upper, n = 10 for the Lower) and the Code 4 Sample (n = 24 for the Upper, n = 3 for the Lower). Data Normalized With Respect to the Coronal Arch Length in Each Dental Arch Were Used; Significance of Mean Difference Was Tested Using the U Values for the Upper and Lower Dental Arch Measures; Z-Values Were Used for the Depths of Dental Arches

Variable	Code 1		Code 4		Significance of Mean Difference
	Mean	S.D.	Mean	S.D.	
Coronal arch width					
Upper					
Central incisors	0.27	0.02	0.28	0.05	NS[a]
Lateral incisors	0.74	0.03	0.82	0.08	**
Canines	1.15	0.05	1.27	0.10	**
First premolars	1.38	0.05	1.61	0.08	**
Second premolars	1.53	0.06	1.82	0.07	**
First molars	1.70	0.05	2.04	0.08	**
Second molars	1.83	0.10	2.20	0.14	**
Lower					
Central incisors	0.17	0.02	0.19	0.03	NS
Lateral incisors	0.57	0.02	0.67	0.04	**
Canines	0.97	0.04	1.18	0.01	**
First premolars	1.27	0.06	1.55	0.07	**
Second premolars	1.46	0.07	1.84	0.07	**
First molars	1.69	0.07	2.20	0.10	**
Second molars	1.88	0.08	2.47	0.09	**
Basal arch width					
Upper					
Interpremolar	1.38	0.09	1.61	0.09	**
Intermolar	1.80	0.07	2.12	0.07	**
Lower					
Interpremolar	1.30	0.10	1.55	0.08	**
Intermolar	1.80	0.11	2.23	0.10	**
Depth of dental arch					
Upper	0.03	0.02	0.02	0.02	NS
Lower	0.05	0.02	0.05	0.03	NS

[a] NS, not statistically significant.
** Statistically significant at the $P = .01$ level.

function, such as a catenary or a polynomial curve. In contrast, We posed the questions: 1) can we justify, on the basis of mathematical rationale, classifying normal dental arch forms into several clusters according to the similarity/dissimilarity of their overall geometric patterns without a subjective visual judgment; if so, 2) how many categorized patterns are there; and 3) what are the patterns?

By a simple visual inspection of the arch form patterns that were coded and illustrated in Figure 2a and b, it is clear that, among all the five code settings, there was a gradual opening of the posterior interarch width that distinguished one coded pattern. This gradual increase was not a geometric effect caused by a normalization of the arch form data relative to the coronal arch length. In fact, there was

complete freedom in the distribution of FA points in the lateral direction. For instance, it is theoretically possible for multiple codes to show a combination of arch forms that cross each other when superimposed on the occlusal plane.

This is the first report that quantitatively and objectively classified arch wire blank forms into four representative codes to maximize the difference between the patterns. We had assumed that there might be specific teeth or tooth segments requiring different weighting coefficients. For example, the canine positions were assumed to play a specific role in characterizing the dental arch wire blank form. Thorough heuristic computation of all combinations of weights led us to reject this assumption because we could not find specific weights on specific FA points.

Agreeing with anatomic dental arch forms in previous studies,[11,15] the dental arch wire blank forms computed for each of the four codes exhibited the best fit with the fourth-order polynomials.

The four coded arch forms may or may not fit with our conventional understanding of dental arch forms or arch wire blank forms, such as squared, oval, or U-shaped arches, possibly because our recognition of a classic arch form is imprecise or because characteristic patterns may strike a strong chord in our memory regardless of our experiences. As noted previously, the coronal arch widths differed significantly between the codes posterior to the lateral incisors in both the upper and lower arches. The patterns of the arch wire blanks were characterized by a gradual increase in difference of arch widths posterior to the lateral incisors. Figure 4 exemplifies comparisons of the code 1 and code 4 out of the four coded samples expressed in actual size. Therefore, some codes may match well with the classic arch wire blank forms and others may be very different.

We determined also that the coordination between both dental arches only allows a subtle variation of 0.3 to 0.4 mm, with almost consistent lateral gaps of about 4.3 mm between the opposing canines and 2.5 mm between the molar teeth. These values might offer a standard for making correct arch wire coordination to achieve proper alignment and tight interdigitation of teeth.

In both the maxilla and mandible, narrower dental arches tended to show a longer coronal arch length while wider arches were associated with shorter lengths. A possible reason for this phenomenon may be that dental arches with shorter coronal arch lengths are accompanied by shorter mesiodistal crown widths. We rejected this possibility because the mesiodistal crown diameters did not differ significantly between code 1 and code 4. Alternatively, the molars are tipped mesially due to the shortness of the skeletal units, which increases vertically the curved line of occlusion and shortens the coronal arch lengths. However, the vertical depths of the dental arches on the sagittal plane did not differ significantly between code 1 and code 4 arch forms. The longer coronal arch length determined for code
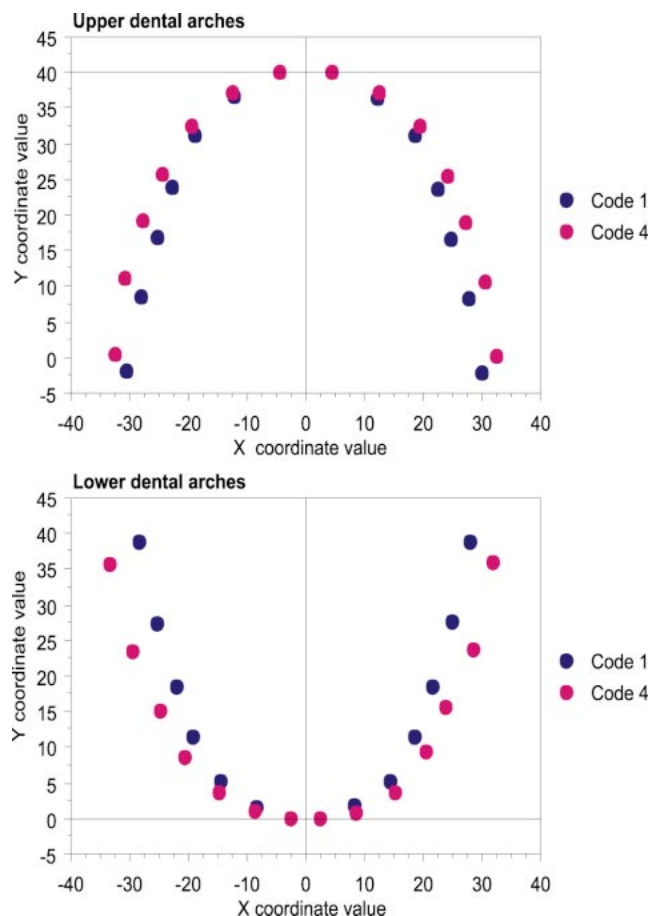

FIGURE 4. Computer plots of code 1 and code 4 dental arch forms expressed in actual size.

4 was not a geometric effect caused in the vertical direction by large teeth crowns or shallow or flatter arch curves.

A third possibility is that there was inadequate space for the teeth so they flared out naturally to fill the space available. The basal interarch widths of the code 4 at the posterior region exhibiting the broadest dental arches were significantly wider than those of code 1. The result therefore suggests that teeth are aligned along the line of the skeletal base posteriorly in individuals with a normal occlusion. One may argue this by contrasting with a concept of influences of soft tissues on skeletal forms.

The dental arch width is dependent on the width of the skeletal basal structure and on the mediolateral positions of teeth within the bone. The width of the skeletal unit, like the tongue and other soft tissues, is defined in part by genetic factors and in part by modification factors such as the elasticity of the surrounding soft tissues.[16] In normal growth, the size of the jaw increases in association with the increases in size of the tongue and other soft tissues.[17–19] Tooth positions within the bone in the mediolateral direction are influenced mainly by soft tissue elasticity located medially and laterally on the skeletal unit influencing on positions of tooth crowns and by the anatomy of cortical

plates that constrain positions of tooth roots. The concept of equilibrium between forces that are directed facially and lingually across the dental arch during normal function is established.[20] Light but long-duration forces from lips and cheeks and from the tongue at rest are important factors in modifying positions of tooth crowns,[16] providing the roots remain mediolaterally within the cortical bone. In a previous study using computed tomography images,[21] the shape (but not size) of the mandible was associated with the alignment of root apices but not with the coronal alignment of the teeth. Our results identified the association between the widths of the dental arch and the adjacent skeletal unit to explain the association between the size (but not the shape) of the arches when the occlusion was normal. Finally, practical significance of the present finding is that the posterior basal arch width can be used as a marker for choosing appropriate arch blanks for edgewise treatment.

CONCLUSIONS

Dental arch wire blank forms were quantified using the teeth's FA points in human adults with normal occlusions. Vector quantization determined that classifying dental arch wire blank forms into four representative codes was optimum to maximize the difference in arch wire blank forms. The classified patterns were differentiated by a gradual broadening of the interarch widths posterior to the lateral incisors. The code with the narrowest arch width had the longest coronal arch length, whereas the code with the widest arch width had the shortest coronal arch length. The interpremolar and intermolar basal arch widths determined for the code with the widest arch width were significantly greater than those having the narrowest width.

We determined that the association between the upper and lower dental arches did not vary by more than 0.3 mm but showed consistent lateral gaps of about 4.3 mm for the opposing canines and 2.8 mm for the molars.

ACKNOWLEDGMENTS

REFERENCES

1. Andrews LF. *Composites. I: Straight-Wire, the Concept and Appliance.* San Diego, Calif: L. A. Wells; 1989:13–33.
2. Angle EH. Classification of malocclusion. *Dent Cosmos.* 1899; 41:248–264.
3. Currier JH. A computerized geometric analysis of human dental arch form. *Am J Orthod.* 1969;56:164–179.
4. MacConail MA, Scher EA. Ideal form of the human dental arcade with some prosthetic applications. *J Dent Res.* 1949;69:285–302.
5. Sampton PD. Dental arch shape: a statistical analysis using conic sections. *Am J Orthod.* 1981;79:535–548.
6. Biggerstaff RH. Three variations in dental arch form estimated by a quadratic equation. *J Dent Res.* 1972;51:1509.
7. BeGole EA. Application of the cubic spline function in the description of dental arch form. *J Dent Res.* 1980;59:1549–1556.
8. Barun S, Hnat WP, Fender DE, Legan HL. The form of the human dental arch. *Angle Orthod.* 1998;68:29–35.
9. Uzuka S, Arai K, Ishikawa H. Polynomial curve superimpositions on dental arch forms with normal occlusions. *Orthod Waves.* [in Japanese] 2000;59:32–42.
10. Kuroda T, Motohashi N, Tominaga R, Iwata K. Three-dimensional dental cast analyzing system using laser scanning. *Am J Orthod Dentofac Orthop.* 1996;110:365–369.
11. Hirogaki Y, Sohmura T, Takahashi J, Noro T, Takada K. Construction of 3D shape of orthodontic dental casts measured from two directions. *Dent Mater J.* 1998;17:115–124.
12. Chang PC, Gray RM. Gradient algorithms for designing predictive vector quantizers. *IEEE Trans Acoust Speech Signal Process.* 1986;34:679–690.
13. Linde Y, Buzo A, Gray RM. An algorithm for vector quantizer design. *IEEE Trans Commun.* 1980;28:84–95.
14. Ballard CF, Wayman JB. A report on a survey of the orthodontic requirements of 310 army apprentices. *Trans Br Soc Study Orthod.* 1964;81–86.
15. Lu KH. An orthogonal analysis of the form symmetry and asymmetry of the dental arch. *Arch Oral Biol.* 1966;11:1057–1069.
16. Proffit WR. Equilibrium theory revisited. *Angle Orthod.* 1978;48: 175–186.
17. Toyoura H. A study on the Japanese tongues: their weight and size. *Hokuetsu Medical J.* [in Japanese] 1934;49:1808–1812.
18. Hopkin GB. Neonatal adult tongue dimensions. *Angle Orthod.* 1967;37:132–133.
19. Cohen AM, Vig S. A serial growth study of the tongue and intermaxillary space. *Angle Orthod.* 1976;46:332–337.
20. Weinstein S, Haack DC, Morris LY, Snyder BB, Attaway HE. On an equilibrium theory of tooth positions. *Angle Orthod.* 1963;33: 1–26.
21. Oda Y. Mandibular apical base form and arrangement of the teeth: mathematical modeling and canonical correlations. *J Osaka Univ Dent Soc.* [in Japanese] 1988;33:145–167.

APPENDIX

Each dental arch form projected onto the occlusal plane was expressed by the X and Y-coordinates of the 14 FA points that were normalized with respect to the coronal arch length, thus generating a 28-dimensional vector. Given that T expresses a code vector, the similarity between the vectors is expressed by as

$$T(X, Q) = \sum_{j=1}^{28} \sqrt{(Xj - Oj)^2},$$

where X represents the input vector and Q designates the quantized vector. Xj is the input vector, where j takes values from 1 to 28, and Qj designates quantized vectors having elements from 1 to 28.

In the present study, calculations were made to classify each set of the upper and lower dentitions into two, three, four, five, and six subcategories (code sets), ie, two to six code vectors. Here we give the computation procedure by exemplifying classification into three code sets.

First, three code vectors were determined out of the 79 points (a collection of vectorized 79 dental arches). The three code vectors were selected according to a criterion that they were located farthest from each other when compared with remaining combinations of interpoint distances and termed as initial code vectors 1, 2, and 3. Second, distances between each point (representing 1 of the 79 dental arch forms) and the three initial code vectors were computed, thus giving each sample point three distances for each respective three initial code vectors. Each point was then categorized into a subcategory that corresponded with the initial code vector that showed the shortest distance with the points.

Geometric centers (the center of gravity) were calculated for each subcategory. The geometric centers D1, D2, and D3 for each of the three subsets thus obtained were assumed as a new set of code vectors. Distances between each sample point and D1, D2, and D3 were computed to pro-

vide three new subsets. The calculation was repeated until the average deviation showed the minimum decremental rates when the optimum number of code sets was determined. The average deviation designates the closeness of a vector that represents a dental arch form to a code vector to which the dental arch form belongs. In other words, the smaller the average deviation value, the higher the accuracy of classification. The smaller the average deviation value was, the closer was the distance between the vector and its belonging code vector. In short,

$$\text{Average deviation} = \frac{\sum\limits_{i=1}^{79} \dfrac{\sum\limits_{j=1}^{28} \sqrt{(Xij - Qj)^2}}{28}}{79}$$

where Xij represents the coordinate values of the jth tooth of the ith dental casts, whereas Qj designates the coordinate values of the jth tooth of the corresponding code vector.